UC San Diego
UC San Diego Previously Published Works

Title
Observations of divergence and upwelling around Point Loma, California,

Permalink

Journal

Author
Roughan, M

Publication Date
2005

DOI

Peer reviewed

Observations of Divergence and Upwelling around Pt Loma, California.

Moninya Roughan[†], Eric J. Terrill, John L. Largier[‡], Mark P. Otero

Scripps Institution of Oceanography, University of California, San Diego, USA.

[†]Corresponding author. Scripps Institution of Oceanography, UCSD, 9500 Gilman Drive, USA 92093-0218. Email:mroughan@ucsd.edu

[‡]Now at Bodega Marine Laboratory, University of California, Davis, USA

Abstract

Historical records of near-surface water temperatures in the southern California Bight often show a preferential cooling in the lee of headlands such as Pt Dume, Palos Verdes and Pt Loma. At times this cooler water is associated with an increase in chlorophyll-a as is evident in satellite images of ocean color from the region. Here we combine hydrographic data from a one day cruise aboard the *RV Roger Revelle* (a precursor to the 0304 CalCOFI cruise) with HF radar (CODAR) measurements, satellite images and long term thermistor records of near-surface temperature to identify a small-scale, isolated upwelling in the lee of Pt Loma (32.5°N). Associated with the more saline water downstream of the headland are higher nutrient concentrations, an increase in chlorophyll-a concentration, and a bloom of chain-forming diatoms, indicative of a mature upwelling system. It is suggested that this upwelling is not primarily due to local or remote wind forcing, but rather the divergence of the prevailing southerly flow as it passes the Pt Loma headland. Time series of surface vorticity calculated from HF radar measurements of sea surface velocity show that as the flow separates from the headland relative vorticity increases offshore of the cape. Inshore the time series of divergence/convergence shows a tendency towards divergence at the surface indicating a preferential upwelling, which appears to raise the thermocline thus resulting in a flux of cold nutrient rich water to the surface. In the presence of high nutrients and light, photosynthetic organisms bloom in these upwelled waters as they are advected away from the headland and offshore by the prevailing surface currents.

1 Introduction

Typically satellite images of sea surface temperature (SST) along the Californian coast such as that shown in Figure 1 reveal large areas of colder (upwelled) water extending along the central and northern Californian coast ($34.5 - 36°$N), particularly during the summer upwelling season. Also depicted in the image are smaller regions of cold, upwelled water in the lee of headlands in the southern Californian Bight (SCB), such as Pt Dume ($34°$N), Palos Verdes ($33.2°$N) and Pt Loma ($32.7°$N). Associated with these cooler upwelled waters in the lee of the headlands are regions of higher chlorophyll-a concentrations. These isolated regions of upwelled water are locally significant in terms of the occurrence of algal blooms, the dispersal of eggs, larvae, and spores and the onshore transport of pollutants from wastewater outfalls (Noble et al., 2004; Boehm et al., 2002). Furthermore, it is possible that associated with the localized upwelling is a more widespread shoaling of the thermocline without surface expression.

Long-term near-surface temperature records obtained from the coastal monitoring program along the San Diego coastline show a preferential cooling in the lee of Pt Loma under certain conditions, where the lee is defined as the region south-eastward of the Pt Loma headland in the 'Coronado Embayment' (Figure 2), (which is also downstream during southerly current events). Figure 3 shows an 18 month record of hourly mean temperatures (Jan 2001−Sept 2002) from 2 sites upstream of the Pt Loma headland (Sunset Cliffs (T1) and Pt Loma (T2)) and 3 sites from within the 'Coronado Embayment' in the lee of Pt Loma (Zuniga Pt (T3), Military Tower (T4) and Imperial Beach (T5)) as indicated in Figure 2, where gaps in the data occur due to instrument loss (e.g. T2, March - June 2002). The time series shows an obvious seasonal trend with an annual temperature range of up to $10°$C. During the winter months (Nov 2001−Feb 2002) surface temperatures were homogeneous across the region (mean $\sim 14°$C) and fluctuations were coherent.

In contrast to this, during the spring and summer months there is an obvious lack of coherence between the waters upstream of Pt Loma and those in the lee of the headland. At times throughout the summer, the waters upstream of the headland were up to $6°$C warmer than those downstream. From May − September 2002 mean surface temperatures increased from $14 - 20°$C indicating a seasonal warming, however during each of these months notable cold water (upwelling) events are observed downstream of Pt Loma. In each case the surface temperature decreased by up to $6°$C. This cooling is most pronounced at Zuniga Pt (T3, immediately in the lee of Pt Loma) where in every occurrence the surface temperatures decreased below the mean winter temperature ($< 14°$C). Throughout each of these periods surface temperatures upstream of Pt Loma either remained constant or continued to increase.

Previously Lentz and Winant (1986) and Hickey et al. (2003) described the low mode coastal trapped waves (CTWs) that propagate through the SCB. These CTWs are generated along the coast of Baja California (Mexico) many hundreds of kilometers to the south. Pringle and Riser (2003) took this work one step further and correlated changes in temperature in the kelp forest north of Pt Loma to remote wind forcing along the Baja coast over 300 km away. The thermistor strings on which they based their temperature analysis were on a single across-shore transect in the Pt Loma kelp forest, approximately 5 km to the north of the tip of Pt Loma (halfway between the Sunset Cliffs (T1) and Pt Loma (T2) thermistors shown in Figure 2). Without the benefit of local velocity measurements, Pringle and Riser (2003) speculated that periods of widespread decrease in temperature were associated with the northward propagation of coastally trapped waves through the region, and discounted the effects of local topography.

The structure of flow around headlands has received limited attention in the southern California Bight, however recent papers by Penven et al. (2000), Dale and Barth (2001), Gan and Allen (2002a, 2002b) discuss aspects of equatorward flow past headlands in wind-forced upwelling regions; and a number of earlier papers e.g. (Wolanski and Heron, 1984) and (Pattiaratchi et al., 1987) discuss flow patterns in the wake of islands. In the presence of thermal stratification, downstream flow structures and mixing often lead to the observation of coldest waters at the tip of the headland where alongshore flow separates from the shore. In general, vorticity balances are best used to compare the effects of upstream shear, the effect of flow across isobaths, flow curvature, and frictional dissipation in control of flow patterns and surface divergence e.g. Penven et al. (2000). While the flow may remain attached to the shoreline (on the one extreme), or shed cyclonic eddies (on the other extreme), the more usual scenario is that of a wake feature such as an attached cyclonic eddy or flow curvature developing downstream of the cape. Topographic upwelling may occur specifically at a cape, either through (i) localized divergence at the tip of the headland (< 10 km) where entrainment into the detached boundary layer leads to divergence inshore of the point of separation, and/or (ii) divergence that extends further downstream ($10 - 100$ km) along the shear zone between the inertial overshoot of the core of the alongshore flow and flows that curve into the embayment. Further, while alongshore patterns in wind forcing may not dominate in the SCB, the topographically driven flow and upwelling patterns may still be modified by spatial patterns of wind stress that are also topographic, resulting in either sheltered areas or areas of enhanced wind forcing. In addition to enhancing or counteracting upwelling effects, where surface wind stress is strong, it may drive vertical mixing across near-surface thermoclines (Caldeira and Marchiesello, 2002).

Here we present observations of the circulation and hydrography during an isolated cool-

ing event in the lee of Pt Loma that occurred in April 2003 and we hypothesize as to how and why the cooling occurs. A full outline of the field program is presented in the following section along with a description of the environmental conditions preceding a 1-day hydrographic survey. In Section 3 the observations are presented, which includes HF radar measurements of surface velocities and hydrographic data, (both continuous underway sampling as well as discrete vertical casts) obtained on 3 April 2003. In Section 4 surface velocity maps and time series of vorticity and divergence/convergence obtained from HF radar measurements of surface velocities are presented. Several upwelling mechanisms are examined by way of explanation, a case for current driven upwelling around Pt Loma is presented and local implications are discussed.

2   The Experimental Setting

The study site extends along the southern Californian coastline from Del Mar (33°N) to the Tijuana River at the Mexican Border (32.5°N) and from the coast to a depth of $\sim$ 150 m. The coastline in this region is generally orientated in a north-south direction (Figure 1) which contrasts to the main SCB where the coastline extends south-eastward away from Pt Conception to south of Dana Pt (33.4°N).

On 3 April 2003 (local time) a one-day cruise was conducted aboard the *RV Roger Revelle* prior to the regular Californian Cooperative Oceanic Fisheries Investigations (CalCOFI) April cruise (Venrick et al., 2003), in the region offshore from Pt Loma (32.5 − 33°N). One aim of the cruise was to study the effect of the Pt Loma headland on the near-shore oceanography of the region, in particular to identify the flow pattern associated with Pt Loma and to differentiate between water-masses found in the 'Coronado Embayment' in the lee of Pt Loma and those found further offshore. The cruise facilitated a large scale hydrographic survey, which included vertical profiles of conductivity, temperature and depth (CTD), nutrients (such as nitrates, phosphates, silicates), and chlorophyll-a, as well as continuous underway thermosalinograph sampling. Net tows were taken for estimates of phytoplankton and zooplankton biomass along transect lines extending offshore from the 30 m isobath. This was combined with a CTD grid and acoustic Doppler current profiler (ADCP) survey from a small boat (a 13' Boston whaler) which was launched from the *Revelle* and operated inshore to the 20 m isobath (Figure 2).

The hydrographic data obtained during the large scale survey of the 0304 CalCOFI cruise indicates that the main axis of the California Current was located well offshore and was not impacting the Pt Loma region (Venrick et al., 2003). Inshore a cyclonic eddy was located in the vicinity of the Channel Islands, and anomalously cold water with high salinities extended

along the coast south of Santa Barbara. Also present were high chlorophyll-a concentrations (up to 8 mg m^{-3}) which Venrick et al. (2003) attributes to stronger than normal upwelling in the Californian Current throughout the season.

In the week leading up to the cruise local winds were light ($1 - 2$ ms^{-1}) and variable which is typical of the region (Lentz and Winant, 1986). Figure 4 shows the along (v, positive northward) and across-shore (u, positive onshore) wind stress measured at Scripps Pier in La Jolla for the 7 days spanning the sampling period. Stress was weak (~ 0.05 Pa) and directed onshore in the lead up to the sampling period and increased, fluctuating to offshore post sampling. The alongshore component was weak and variable, although tended equatorward in this period.

The tidal range in San Diego Bay is ~ 1.7 m from mean lower-low to mean higher-high water, with extreme ranges being up to 3 m. On the day of the cruise the semi-diurnal tide had a range of ~ 1 m, the high tide (1.3 m) at 18:00 UTC corresponded with the start of cruise, with the tide ebbing throughout the sampling period with a low of 0.25 m at 23:45 UTC (hereafter all times are in UTC). Chadwick and Largier (1999a, 1999b) found that in general tidal outflow from San Diego Bay creates a plume that extends up to 2 km south of the mouth with associated velocities of $10 - 20$ cms^{-1}. This outflow from San Diego Bay may have had some small influence on CTD station C8 (Figure 2) at the start of the cruise (where the observed outflow was warmer than the surrounding waters). However, as the pattern of interest here is one of cold surface waters and the extent of bay outflow is limited to within a short distance from the mouth of the bay, the bay outflow is not considered important at this time.

3 Field Observations

3.1 Surface Velocities

Surface velocities were obtained from the San Diego Coastal Ocean Observing System (SD-COOS: http://www.sdcoos.ucsd.edu) HF radar (CODAR) array. The positions of the CO-DAR instruments are shown in Figure 2, the first on the Pt Loma headland, the second is near Imperial Beach, the third instrument is located on Coronado Island which lies south-west of our domain, immediately south of the Mexican Border and the fourth CODAR unit, owned by CICESE/UABC, is sited at the PEMEX facility in Rosarito Beach, Mexico.

The four systems operate at a nominal transmit frequency of 25 MHz which results in the interpretation of Doppler shifts by ocean currents via a scattered signal from Bragg wavelengths (λ) of approximately 6 m. The four sites each report 1 km resolution radial vectors

4

on an hourly basis and these are combined to a yield a total vector solution (velocities) for the entire domain, which are archived, and distributed in near real time on the internet. Due to the Bragg scatter dependence of the HF radar current measuring technique, the measured currents may extend to depths of approximately $\lambda/2\pi$ to $\lambda/4\pi$ (i.e., less than 1 m), depending on the vertical shear present at the surface (Stewart and Joy, 1974). Observations from CODAR arrays along the Californian coastline have proved to be reliable representations of the surface flow-field (Paduan and Cook, 1997; Kaplan et al., 2004). Likewise, preliminary quality control and ground-truthing of CODAR data in this region indicate that CODAR data reasonably represent the near-surface flow patterns in this region. While the HF radar directly measures surface currents (1 m or less), we found the near-surface velocities compare favorably with barotropic velocities obtained inshore during the small boat ADCP survey. The vertical ADCP profiles revealed the low-shear, barotropic nature of the flow at water depths less than 20 m within the 'Coronado Embayment' under such southerly flow conditions which give weight to the assumption that the CODAR-derived surface velocity field represent the flow throughout the water column inshore at this time.

The CODAR velocity fields (Figure 5) are overlayed on mean satellite images of SST (left) and ocean color (right) at 300 m resolution on 3 April 2003, where the surface CODAR velocities are a 24 h average centered on the time of the satellite pass. Generally the flow field was southerly offshore and weak and variable in direction in the lee of Pt Loma (within the 'Coronado Embayment'). The flow pattern depicts strong cyclonic flow around Pt Loma (up to 40 cms^{-1}) which extends up to 10 km offshore (where each vector on the CODAR map represents a 24 h average over a ~ 1 km^2 region). This pattern is observed for several days prior to the sampling period. Approximately 10 km downstream of the cape the flow converges and tends directly southward offshore of the 'Coronado embayment'.

Empirical orthogonal function analysis of current meter data from $1986 - 1988$ revealed two dominant flow patterns in the region and that the first two modes of variability accounted for approximately 87% of the non-tidal variance in the region (Hendricks and Christensen, 1987). The first mode ($\sim 64\%$) revealed a dominant alongcoast flow which was southward the majority of the time, while the second mode ($\sim 23\%$) was dominated by a sheared across-shore flow with a recirculating eddy to the south of the region extending $10 - 15$ km offshore. The eddy tended to be counter-clockwise although clockwise rotation was also observed and southward along coast flow was a maximum in the spring time (i.e. during our study period). Both of these flow patterns have been observed in the CODAR data, however during our study period it is the first mode (southward) flow which is seen in the surface velocity fields.

The fusion of the HF radar data with the satellite imagery illustrates the interplay be-

tween the dynamics and the physical and biological observations. In Figure 5 the surface velocity patterns align with SST and chlorophyll-a patterns: warm waters are associated with the stronger velocities west of Pt Loma and low chlorophyll-a concentrations. The cooler waters in the lee of Pt Loma have weaker surface velocities and higher concentrations of chlorophyll-a.

3.2   Hydrography

Spatial maps of temperature (T), salinity (S), density (ρ), nitrate (N), dissolved oxygen (DO) and chlorophyll-a (F) at a depth of 10 m from the CTD casts and water samples obtained from the *RV Roger Revelle* on $3-4$ April 2003 are shown in Figure 6. The figure clearly shows the presence of colder, more saline, nutrient-rich water in the lee of Pt Loma (T $= 12.5°$C, S $= 33.6$ psu, N $= 11$ μmolL^{-1}). This water is more dense than the water offshore ($\rho = 25.4$ kg m^{-3}) and has a low dissolved oxygen content (DO $= 4$ mlL^{-1}) and chlorophyll-a concentration (F $= 10$ mg m^{-3}). Qualitatively the surface measurements of chlorophyll-a (Figure 6 f) agree with remotely sensed estimates (Figure 5), both of which show the location of the chlorophyll-a maximum directly at, and in the lee of Pt Loma.

Continuous underway sampling of temperature, salinity, dissolved oxygen, and fluorescence was also conducted aboard the *Revelle* through a water intake at a depth of 5 m. Surface maps of derived density and fluorescence (Figure 7 a,b) confirm the presence of more dense water at a depth of 5 m both in the lee of Pt Loma and directly adjacent to the point, associated with a region of higher F concentration (note that the extension of cool salty water north of Pt Loma is likely an artifact of the contouring routine). The underway sampling shows the shape of the plume of high ρ and F water and its extension southward away from Pt Loma. Overlayed on the underway data are CODAR surface velocity maps which indicate the relationship between the surface velocities and the high density plume. F concentration increases with distance from the headland consistent with an active bloom i.e. *in situ* production in ageing waters. While maps of surface properties (not shown) reveal more uniform temperature and salinity (S $= 33.3-33.5$ psu, T $= 14-15.5°$C), the surface chlorophyll-a maximum is still evident in the lee of Pt Loma (F $= 8$ mg m^{-3}).

A distinct difference was found between the waters of the 'Coronado Embayment' and the waters offshore. This is evident in the temperature, salinity and chlorophyll-a concentrations shown in Figure 7 c,d. The T/S/F diagram (Figure 7 c) depicts two distinct surface water-masses, and a third, cooler, more saline deep water-mass. The saltier of the surface water-masses is found in the 'Coronado Embayment' (T$=14-15°$C, S$= > 33.45$ psu), with a surface mixed layer of $3-12$ m (Figure 7 d) and high chlorophyll-a (F $= 6-10$ mg m^{-3}).

This indicates an upwelling of water in the lee of Pt Loma with some warming and 'greening' after it reaches the surface. The phytoplankton assemblage in the plume in the lee of Pt Loma was dominated by chain-forming diatoms (M. Ohman, *Pers. Comm.*), consistent with active upwelling and new production. The second distinct surface water-mass is seen more offshore and it is distinguished by warmer, less saline waters (T = $14.5 - 16$°C, S = $33.25 - 33.4$ psu), in which both nitrate and chlorophyll-*a* concentrations were low (N = 0.5 μmolL^{-1}, F = 1.2 mg m^{-3}, Figure 6 e,f) consistent with an offshore origin in the surface waters of the Californian Current.

The cold waters at the surface immediately south of Pt Loma are distinguished by lower dissolved oxygen concentrations and a downstream increase in fluorescence with warming. These patterns indicate an isolated upwelling source at Pt Loma with cold water streaming southwards from the point, advected by the currents evident in the CODAR data. As the water is advected away from the point, it is subject to solar heating and surface water temperatures increase (T = 15°C), resulting in stratification, while salinity remains high, indicating the upwelled origin of the surface waters. At the same time, fluorescence increases and nutrient concentrations decrease in and above the thermocline.

4 Discussion

The observations presented showing the regional flow patterns and evidence of localized upwelling in the lee of Pt Loma raise three important questions; 1. What is the circulation in the region?, 2. What drives the circulation?, and 3. Does this circulation pattern drive the localized upwelling? The available data are insufficient to answer all three of these questions completely, however having addressed the circulation patterns in the region we now speculate on what drives the circulation and infer that the local circulation does in fact drive the localized upwelling.

4.1 Wind Forcing

Generally local winds in San Diego are light and variable and wind-driven upwelling is not the dominant forcing in the region (Lentz and Winant, 1986; Noble et al., 2004). However, at times the local wind field may interact with the complex topography of the Pt Loma headland in a way that leads to offshore Ekman transport of surface waters. For example, the day prior to the cruise was characterized by onshore wind stress of the order of 0.05 Pa (Figure 4), which can be expected to drive southward Ekman transport of surface waters out of the 'Coronado Embayment'. While this postulated Ekman transport may have contributed

to the upwelling of cold water observed on 3 April, there is no evident correlation between wind and observed flow patterns or surface temperatures, neither in the data analyzed in this study nor in the analysis conducted by Pringle and Riser (2003).

The temperature data from the coastal thermistor array (Figure 3) shows periods where widespread temperature decreases occurred throughout the embayment and to the north of Pt Loma as well (e.g. April-May 2001, July-Aug 2001) and from the evidence of Pringle and Riser (2003) it is possible that this sporadic widespread cooling could be attributed to remotely forced coastal trapped waves. However, clearly there are other cooling events which are restricted to the south of Pt Loma, resulting in a temperature difference of the order of $3 - 5°C$ between sites upstream and downstream of the tip of Pt Loma (e.g. Aug and Oct 2001, May, July and Aug 2002 in Figure 3). During these events the coldest water is found at T3 immediately in the lee of Pt Loma. Further south, waters are a degree warmer, consistent with a center of upwelling at the tip of the cape. Waters to the north of the headland do not undergo cooling. It is these localized upwelling events, restricted to the lee of the Pt Loma headland, that are of interest here.

4.2 Vorticity and Divergence

The surface velocity field obtained from the HF radar array can be used to to investigate the mechanisms behind the upwelling and the dynamics of the flow in the region. The spatially gridded nature of the HF radar current data lends itself to the computation of both relative vorticity (ζ) and divergence from a first difference on a two by two grid where vorticity is estimated as $dv/dx - du/dy$ and divergence as $dv/dy + du/dx$. Figure 8 a shows the relative vorticity of the 24 h averaged flow field centered on 2 April 2003 (24 hours prior to our cruise time), where red (blue) indicates positive (negative) vorticity, (note that the derivatives are computed on the mean flow field).

A region of high positive vorticity (with maximum relative vorticity of $\zeta > 1 \times 10^{-4}\text{s}^{-1}$) is evident directly west and southwest of Pt Loma, where velocities are high, shear is strong and flow exhibits cyclonic curvature. Other than a localized patch of negative relative vorticity at the tip of Pt Loma, there is a trend of decreasing positive vorticity along the detached shear zone that extends south-eastward to intersect the shoreline south of 32.5 °N (where negative vorticity is observed as flow curves to follow the shoreline and then heads offshore). Within the embayment and offshore of the shear zone, vorticity patterns are weaker.

Divergence of the surface flow is estimated from the CODAR surface velocity fields over the same 24 h period and is shown in Figure 8 b. In the figure, blue (red) represents surface divergence (convergence) which indicates upwelling (downwelling). Particularly noticeable is

the blue/upwelling region at the tip of Pt Loma, extending south-eastward into the 'Coronado Embayment', inshore of the vorticity maximum (shear zone). In this region individual grid boxes show maximum divergence over $0.5 \times 10^{-4} s^{-1}$, at a location characterized by near-zero relative vorticity, suggesting that upwelling is not vortex-driven but more associated with divergence in low-vorticity linear flows. This band of high divergence in the 'Coronado Embayment' coincides with the shipboard observation of highest salinity (strongest upwelling) mid-transect. Positive divergence is also observed within the embayment, inshore of the shear zone and the axis of maximum divergence. Specifically, divergence is observed at the tip of Pt Loma in association with entrainment of embayment surface waters by the separating shear zone.

To examine the temporal variability of the vorticity and divergence/convergence in the Pt Loma region, time series are spatially averaged across four different regions (of at least 16 different grid boxes) for the period 24 March − 8 April 2003. The regions were chosen to represent shifts in the dynamics from upstream prior to flow separation, at Pt Loma, and downstream as flow progresses southward. The dots that define the each of the regions (Figure 9) represent corners of the defining grid in which radial vectors are combined to create orthogonal (north/south) vectors. A 24 h sliding average window was applied to the velocity fields prior to computing the divergence and vorticity fields, effectively acting as a lowpass filter on the current data. After computing the dynamical fields over the 1 km grids that define the HF radar observations, spatial averages were computed over the domains shown. While there was some initial concern that outliers of the data may influence the computed means, subsequent computation of the spatial median showed little difference from the means.

The time series of vorticity (Figure 9 a) shows a clear delineation between region 1 (upstream of Pt Loma) and regions $2-4$ (south and southeast of Pt Loma), with positive vorticity ranging $2-7 \times 10^{-5}$ s^{-1} in region 1 and $-2-2 \times 10^{-5}$ s^{-1} in regions $2-4$. This indicates the persistent strong positive vorticity in the southward flow along the shoreline of the Pt Loma headland. The time series of divergence (Figure 9 b) illustrates the tendency for surface convergence in region 1 (upstream of Pt Loma), fluctuations between convergence and divergence in region 2, (at the tip of Pt Loma) and stronger divergence (upwelling) in regions $3-4$ (south and southeast of Pt Loma). There is one period of 1.5 days where there is convergence across the entire region (downwelling favorable). However, immediately prior to this were several days of upwelling. Examination of the time series for the different regions also illustrates the spatial variability present between the regions, supporting the scales of spatial gradients observed in the satellite imagery.

4.3 Upwelling

By continuity, horizontal divergence at the surface results in vertical upwelling of dense/cold water from depth. The region of maximum divergence indicated in Figure 8 coincides with the region of coldest water as seen in the underway data (Figure 7). From vertical CTD casts the mixed layer is estimated to be $8 - 10$ m thick. In the absence of strong surface stress, we expect momentum to be vertically mixed across the surface mixed layer hence CODAR surface velocities can be used to represent surface mixed layer velocities. For illustration, if one chooses a mixed layer depth of 10 m, and a surface divergence of $0.5 - 1.5 \times 10^{-5}$ s^{-1} (from the time series in Figure 9), this results in an upwelling velocity of $5 - 15 \times 10^{-5}$ ms^{-1}, which over a 24 h period would result in a vertical uplift of $4.5 - 13$ m.

The extent of the vertical mixed layer is shown in the CTD casts in Figure 7. The mixed layer can be as shallow as 4 m (inshore) or up to 10 m deep (offshore). The thermocline is thus shallow in this region and has only to be uplifted on the order of a few meters to have a significant effect on the temperature in the surface waters. The T/S properties obtained from the vertical CTD casts near Pt Loma show that the high chlorophyll-a surface waters at the Pt Loma promontory originated at a depth of less than 15 m immediately west of the cape (and deeper depths at stations further offshore) again suggesting a regional uplift of the thermocline that primes the localized upwelling at Pt Loma. Hence the observed divergence in the surface flow field, although small, is sufficient (over a $24 - 48$ h period) to raise sub-thermocline, nutrient-rich water to the surface in $2 - 3$ days, where after phytoplankton blooms can develop. If the divergence persists this could continue to raise the uplifted waters to the surface where these upwelled waters are then warmed as they are advected southward away from Pt Loma.

Figure 9 shows a persistent divergence in regions 3 and 4 for $2 - 8$ April, which coincides well with the observed upwelling patterns on 3 April. This divergence had been notably absent on 1 April, following a weakening of the relative vorticity maximum to the west of Pt Loma (region 1) on 31 March (and a weakening of the southward alongshore flow past Pt Loma). A similar divergence period was observed $25 - 28$ March, but without hydrographic data corroborate the event.

4.3.1 Bathymetric steering

The bathymetry around Pt Loma depicted in Figure 2 shows that the isobaths run shore-parallel upstream of the Pt Loma headland. At the headland the 10 and 25 m isobath follow the topography around the headland whereas the 50 m isobath extends directly southward away from the headland. Southward shore parallel flow along the isobaths would result in a

bathymetric steering around the headland at depths of less than 50 m (due to conservation of vorticity), resulting in divergence inshore of the cape. At depths of greater than 50 m, flow continues southward with possible vortex stretching and convergence. The divergence of the flow field inshore of the cape would drive bottom waters upward. In this way topographic steering of the flow around Pt Loma can result in upwelling observed in the lee of Pt Loma.

Pringle and Riser (2003) presented a scaling analysis based on historical observations of velocities obtained from up to 30 km north of Pt Loma. They state that alongshore velocities are weak (~ 0.1 ms^{-1}) and rotation around Pt Loma is not sufficient to drive upwelling. Local observations of surface velocities obtained from the CODAR array show that surface velocities are up to 0.40 ms^{-1} upstream of Pt Loma i.e. can be up to 4 times greater than those used in the scaling argument of Pringle and Riser (2003). Hence it is possible that under stronger southerly flow conditions rotation of the flow around Pt Loma may be responsible for driving upwelling in the lee of the headland.

4.4   Local Implications

A schematic diagram of the circulation around Pt Loma is shown in Figure 10. The diagram shows the direction of the mean current, southward adjacent to Pt Loma. As the water continues southward past the headland it separates from the coast and a vorticity maximum is observed west of Pt Loma. The flow diverges from the coast at the tip of the headland, leading to upwelling of deeper nutrient-rich cold waters. In this case the water which is upwelled at the tip of the headland is swept south of the headland into the 'Coronado Embayment'. The upwelled waters are high in nutrients and once exposed to light, primary production occurs and phytoplankton blooms develop. As time progresses the upwelled waters are heated slowly, nutrients are taken up, concentrations of chlorophyll-a increase and water is moved downstream away from the headland. The spatial concentrations of density and chlorophyll-a in Figure 7 show the gradual decrease in density (temperature) away from Pt Loma and the increase in Fluorescence. This plume is of order $20-30$ km long corresponding to $1-2$ days of advection in currents with velocities of order 0.15 ms^{-1} in the 'Coronado Embayment'. The plume which forms is a notable region of primary production in the SCB.

It is known that the southern end of the La Jolla kelp forest which is distinguished by cooler temperatures are more species diverse than the northern kelp forest (E. Parnell *Pers. Comm.*). Furthermore the Pt Loma kelp forest is known to be the most persistent and productive along the Californian coastline (Broitman and Kinlan, 2003). It has been shown that the health of the kelp forest is correlated with the influx of cold (nutrient rich) water (Tegner

et al., 1996). In an investigation of chlorophyll-a distributions in eastern boundary currents Thomas et al. (2001) found that near 32°N in the SCB, chlorophyll-a concentrations were considerably lower than those at higher latitudes. However the high concentrations to the north exhibit distinct seasonality whereas in the Pt Loma region chlorophyll-a concentrations displayed a minimum seasonality which further suggests that the presence of upwelling in this region is less dependent on seasonal winds and perhaps more dependent on southward flow past the Pt Loma headland.

The scenario reported here contrasts to that of a typical upwelling shadow as observed behind larger headlands in regions of strong wind-driven upwelling, such as along the northern Californian coast, e.g. in the lee of Cape Mendocino (40.5°N), Pt Reyes (37.8°N) and Monterey Bay (36.8°N) (Graham and Largier, 1997). An upwelling shadow can form as cold water which is upwelled upstream is advected into the lee of the headland and retained where it can stratify (warm) and where phytoplankton blooms develop. The observations from Pt Loma suggest that recirculation, retention and large scale warming do not occur as in the upwelling shadow of northern Monterey Bay. However as the mean southward flow by-passes the embayment, flow through the 'Coronado Embayment' is slower and residence time is longer. This contrasts the small scale retention feature observed at depth in the lee of Bodega Head in northern California, where in the region of strong upwelling the wind driven surface layers are rapidly advected equatorward opposing a return flow at depth (Roughan et al., 2005). In the lee of larger headlands, one may observe large-scale retention and warming deep in the bay, whereas one may also observe coldest waters due to a localized upwelling maximum at the tip of the cape (e.g., Pt Reyes).

Such localized upwelling is also evident in the lee of Smoky Cape in the East Australian Current (Roughan and Middleton, 2004) and in other places along the SCB shoreline, in particular in San Pedro Bay (in the lee of Palos Verdes peninsula) and in the lee of Pt Dume, and it is expected that the same divergence mechanism is the cause of the localized upwelling. Such patterns of small, isolated, yet semi-persistent, upwelling have implications for the production, distribution and retention of planktonic organisms, the transport of larval fish and the location and health of our kelp forests. It is suggested that further attention be given to these small-scale upwelling features.

5   Acknowledgements

References

Boehm, A., B. Sanders, and C. Winant, 2002: Cross-shelf transport at Huntington Beach. implications for the fate of sewage discharged through an offshore ocean outfall. *Environ. Science and Tech.*, **36**, 1899–1906.

Broitman, B. R., and B. P. Kinlan, 2003: A coupled spatial pattern of benthic and pelagic ecosystem structure in coastal upwelling regions. In *Procs: Eastern Pacific Oceanography Conference 2003*.

Caldeira, R. M. A., and P. Marchiesello, 2002: Ocean response to wind sheltering in the Southern California Bight. *Geophys. Res. Letters*, **29 (13)**.

Chadwick, D. B., and J. L. Largier, 1999a: The influence of tidal range on the exchange between San Diego Bay and the ocean. *J. Geophys. Res.*, **104**, 29885–29900.

Chadwick, D. B., and J. L. Largier, 1999b: Tidal exchange at the bay-ocean boundary. *J. Geophys. Res.*, **104**, 29901–29919.

Dale, A. C., and J. A. Barth, 2001: The hydraulics of an evolving upwelling jet flowing around a cape. *J. Phys. Oceanogr.*, **31(1)**, 226–243.

Gan, J., and J. S. Allen, 2002a: A modeling study of shelf circulation off northern California in the region of the Coastal Ocean Dynamics Experiment: Response to relaxation of upwelling winds. *J. Geophys. Res.*, **107 (C9)**, 3123. doi: 10.1029/2000JC000768,2002.

Gan, J., and J. S. Allen, 2002b: A modeling study of shelf circulation off northern California in the region of the Coastal Ocean Dynamics Experiment 2: Simulations and comparisons with observations. *J. Geophys. Res.*, **107 (C11)**, 3184. doi: 10.1029/2000JC001190,2002.

Graham, W. M., and J. L. Largier, 1997: Upwelling shadows as nearshore retention sites: the example of northern Monterey Bay. *Cont. Shelf Res.*, **17**, 509–532.

Hendricks, T. J., and N. Christensen, 1987: Modeling of flow fields and effluent trajectories in the San Diego Bight. Tech. rep., Southern California Coastal Water Research Project.

Hickey, B. M., E. L. Dobbins, and S. E. Allen, 2003: Local and remote forcing of currents and temperature in the southern Californian bight. *J. Geophys. Res.*, **108 (C3)**, 3081. doi:10.1029/2000JC000313.

Kaplan, D. M., J. L. Largier, and L. W. Botsford, 2004: Surface currents along the coast of northern-central California derived from high-frequency radar data. *J. Geophys. Res.*, **in preparation**.

Lentz, S. J., and C. D. Winant, 1986: Subinertial currents on the Southern Californian Shelf. *J. Phys. Oceanogr.*, **16**, 1737–1750.

Noble, M. A., J. Xu, L. Rosenfeld, J. L. Largier, P. Hamilton, B. Jones, and G. Robertson, 2004: Huntington beach shoreline contamination investigations, phase III, final report. Tech. rep., United States Geological Survey. http://pubs.usgs.gov/of/2004/1019/.

Paduan, J. D., and M. S. Cook, 1997: Mapping surface currents in Monterey Bay with CODAR-type HF radar. *Oceanography*, **10**, 49–52.

Pattiaratchi, C., A. James, and M. Collins., 1987: Island wakes and headland eddies; a comparison between remotely-sensed data and laboratory experiments. *J. Geophys. Res.*, **92**, 783–794.

Penven, P., C. Roy, A. Colin, and J. Largier, 2000: Simulation of a coastal jet retention process using a barotropic model. *Oceanologica Acta*, **23(5)**, 615–634.

Pringle, J. M., and K. Riser, 2003: Remotely forced nearshore upwelling in Southern California. *J. Geophys. Res.*, **108 (C4)**. doi:10.1029/2002JC001447.

Roughan, M., A. J. Mace, J. L. Largier, S. G. Morgan, and J. L. Fisher, 2005: Sub-surface recirculation and larval retention in the lee of a small headland: A variation on the upwelling shadow theme. *To submit to J. Geophys. Res.*

Roughan, M., and J. H. Middleton, 2004: On the East Australian Current: Variability, encroachment and upwelling. *J. Geophys. Res.*, **109(C07003)**. doi:10.1029/2003JC001833.

Stewart, R. H., and J. W. Joy, 1974: HF radio measurements of surface currents. *Deep-Sea Res.*, **21**, 1039–1049.

Tegner, M. J., P. K. Dayton, P. B. Edwards, and K. L. Riser, 1996: Is there evidence for long-term climatic change in Southern California kelp forests?. Tech. rep., Calif. Coop. Fish. Invest. Rep.

Thomas, A. C., M. E. Carr, and P. T. Strubb, 2001: Chlorophyll variability in eastern boundary currents. *Geophys. Res. Letters*, **28(18)**, 3421–3424.

Venrick, E., S. J. Bograd, D. Checkley, and R. Durazo, 2003: The state of the Californian Current, $2002 - 2003$: Tropical and subarctic influences vie for dominance. In Harloan, J. (Ed.), *California Cooperative Oceanic Fisheries Investigations Report*, Vol. 44. CalCOFI, La Jolla, California.

Wolanski, E. J. I., and M. L. Heron, 1984: Isladnd wakes in shallow waters. *J. Geophys. Res.*, **89**, 10 553 – 10 569.

List of Figures

Figure 1: Satellite image of sea surface temperature in the southern California Bight (3/10/2002). Note the cooler temperatures in the lee of headlands in the Bight.
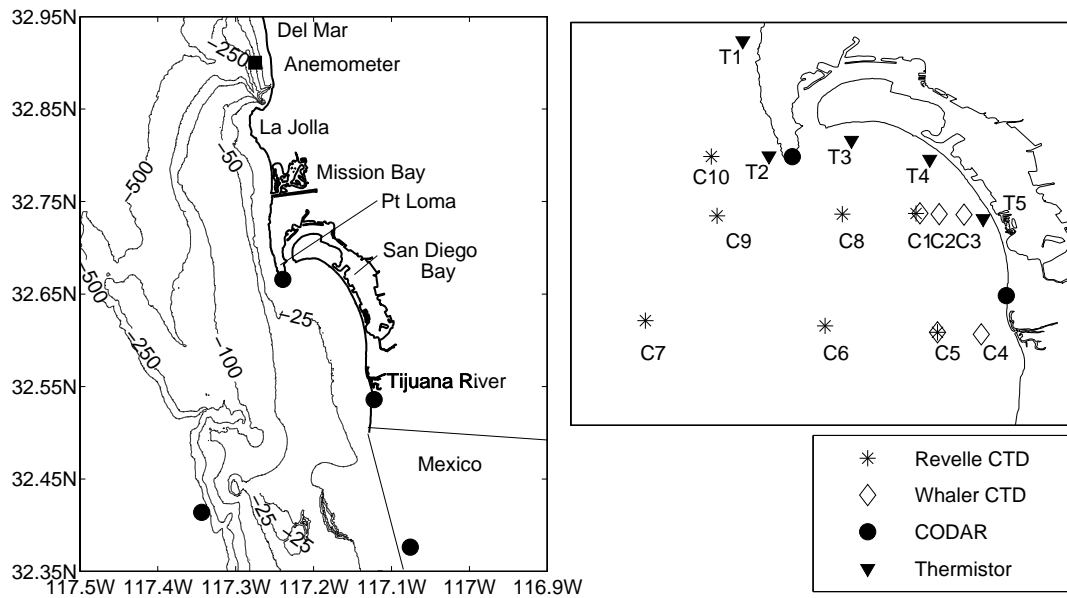
Figure 2: Location of the study site at Pt Loma, California. Instrument and sample locations are indicated as follows: surface thermistor moorings (▼), HF Radar (CODAR) instruments (●), anemometer at La Jolla (■), whaler CTD casts (◇), and Revelle CTD casts (∗).
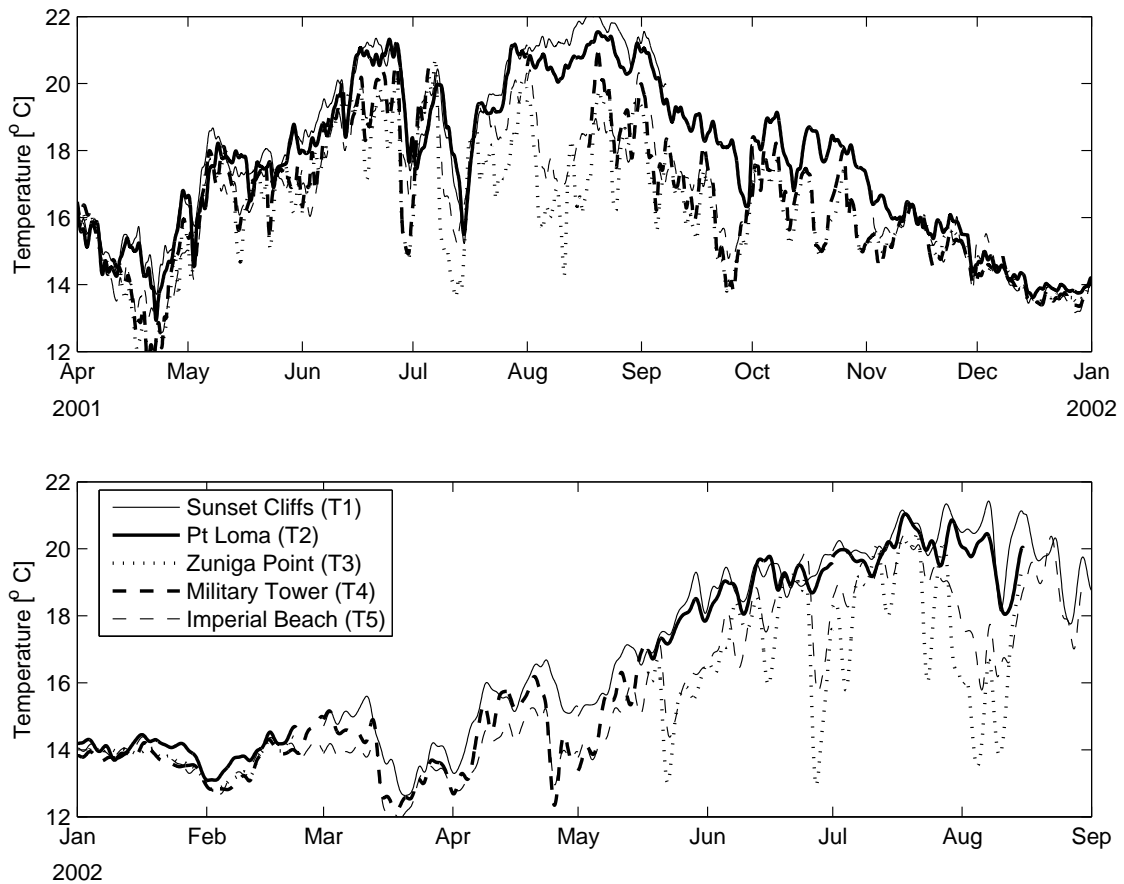
Figure 3: Near-surface temperature from 2 locations upstream of the Pt Loma headland (Sunset Cliffs (T1), Pt Loma (T2)) and 3 locations in the 'Coronado Embayment' (Zuniga Pt (T3), Military Tower (T4) and Imperial Beach (T5)) as indicated in Figure 2, from April − December 2001 (top) and January − September 2002 (bottom). Gaps in the data occur when instruments were lost.
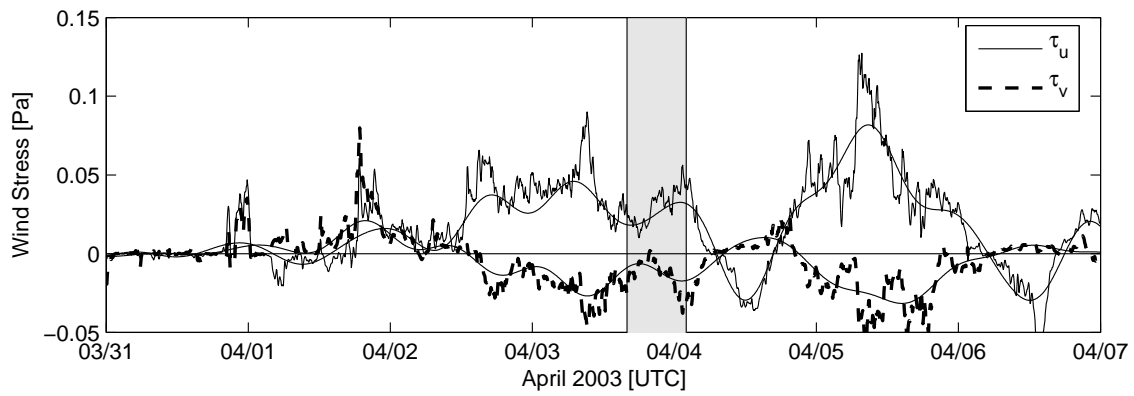
Figure 4: Wind stress (Pa) at La Jolla (Figure 2) in u (positive onshore) and v (positive northward), overlaid with a 12 hour lowpass filter. Dates are in UTC and the sampling period is indicated by the shaded area.
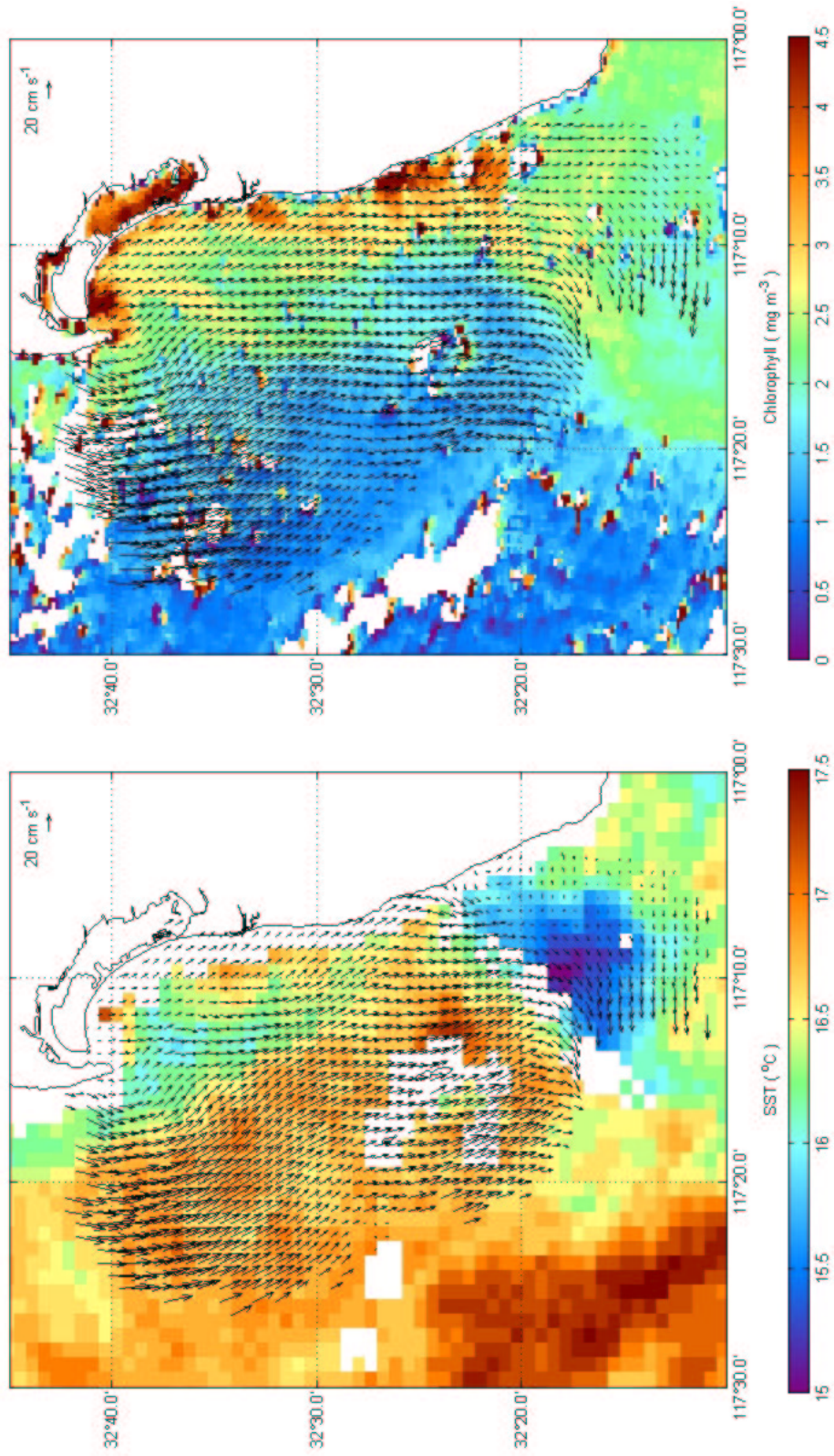
Figure 5: Satellite image of sea surface temperature (left) and ocean color (right) corrected for chlorophyll-*a* concentration. Overlayed on both of these is a 24 h CODAR average of sea surface velocities for 3 April 2003.
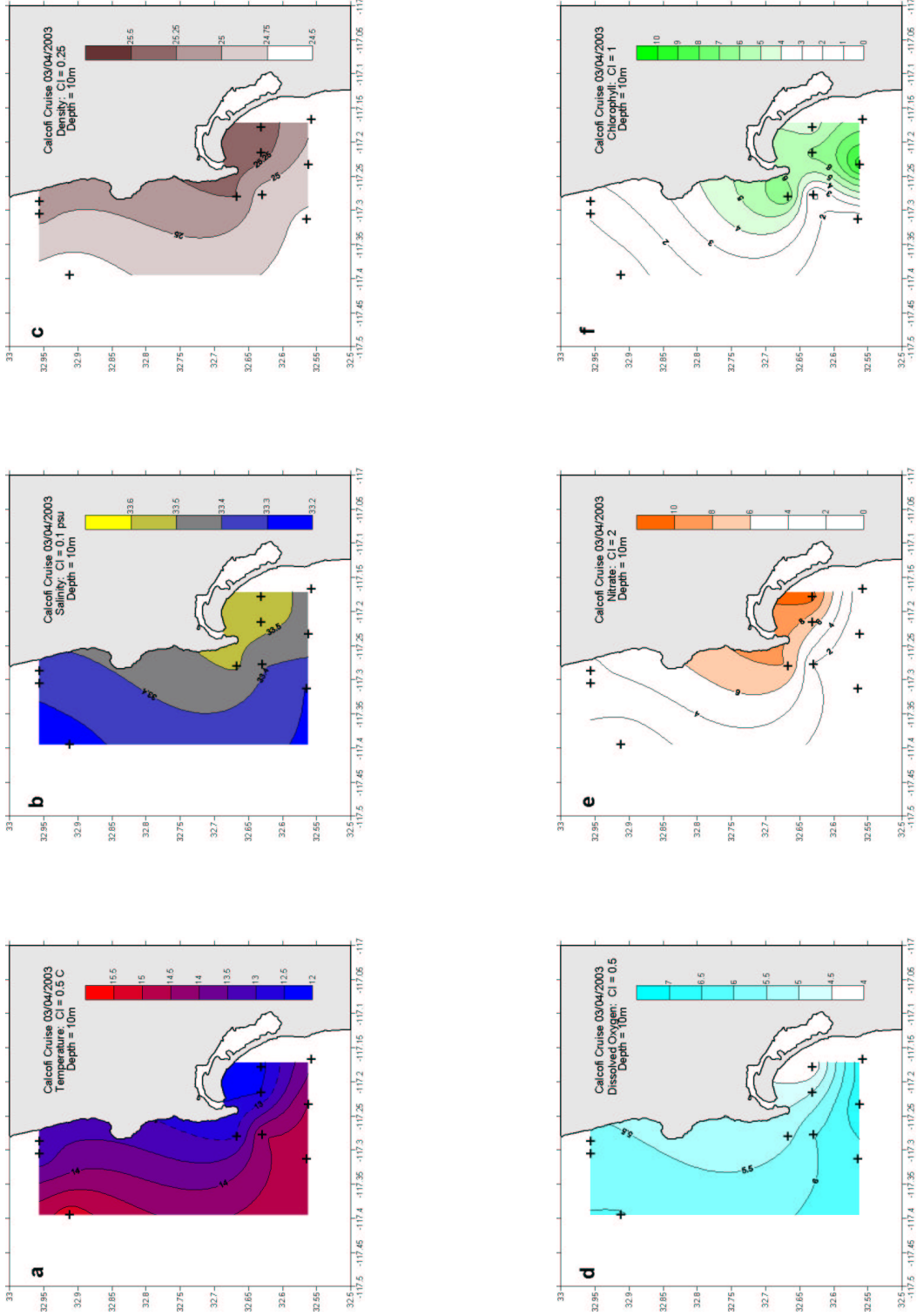
Figure 6: Contour maps of a) Temperature (°C), b) Salinity (psu), c) Density (kg m^{-3}), d) Dissolved Oxygen (mL^{-1}), e) Nitrate (µmol L^{-1}), and f) Chlorophyll-a (mg m^{-3}), at 10 m depth.
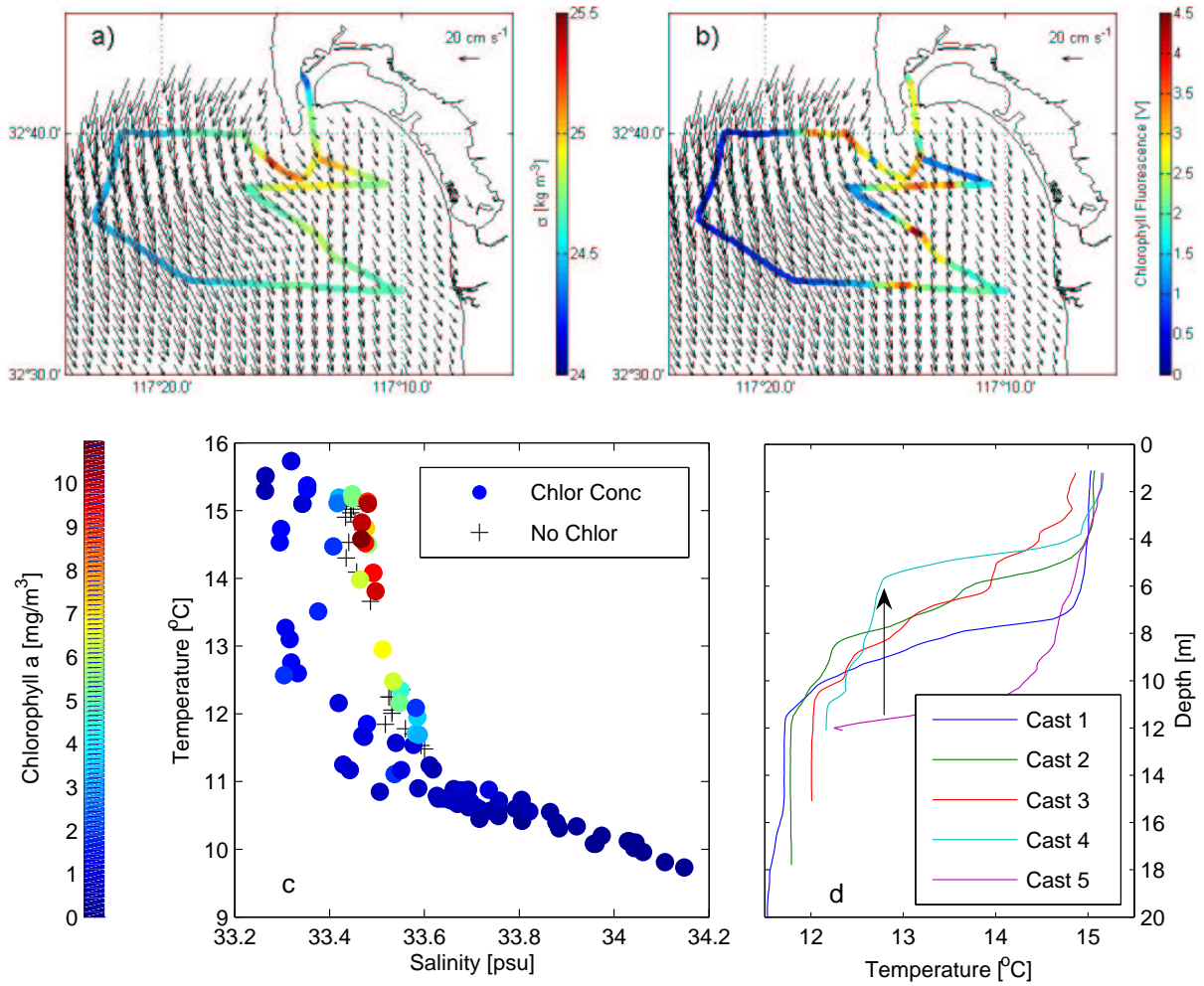
Figure 7: a) Density (kg m^{-3}), and b) fluorescence (Volts) at a depth of 5 m overlayed with CODAR surface velocities. c) Temperature, salinity and chlorophyll-a diagram. The dots represent T and S obtained from the *RV Revelle* CTD casts, and chlorophyll-a concentration is represented by the colorbar. The black + represent T and S at inshore stations obtained from the small boat (no chlorophyll data is available for these stations). d) Vertical temperature profiles from CTD casts. Note the difference in the thermocline depth between casts inshore and offshore indicated by the arrow.
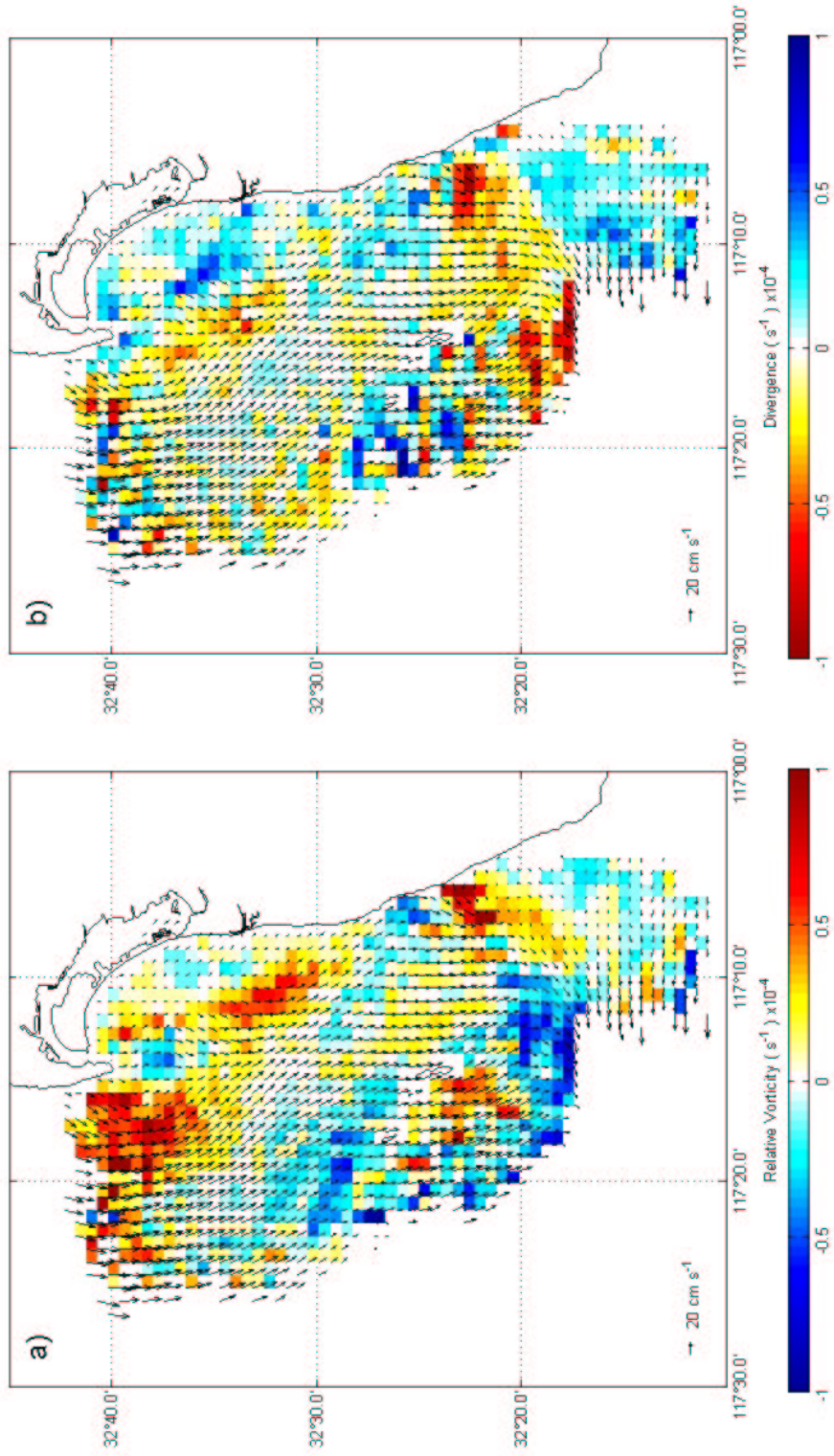
24

Figure 8: a) The relative vorticity ($s^{-1} \times 10^{-4}$) field in the Coronado Embayment calculated from a 24 hour average of the CODAR surface velocities centered on 2 April 2003. Red (blue) shading represents a positive (negative) vorticity and white is neutral. b) The divergence/convergence ($s^{-1} \times 10^{-4}$) field in the Coronado Embayment calculated from the same CODAR surface velocities. Blue (red) shading represents divergence (convergence) indicating upwelling (downwelling), and white is neutral.
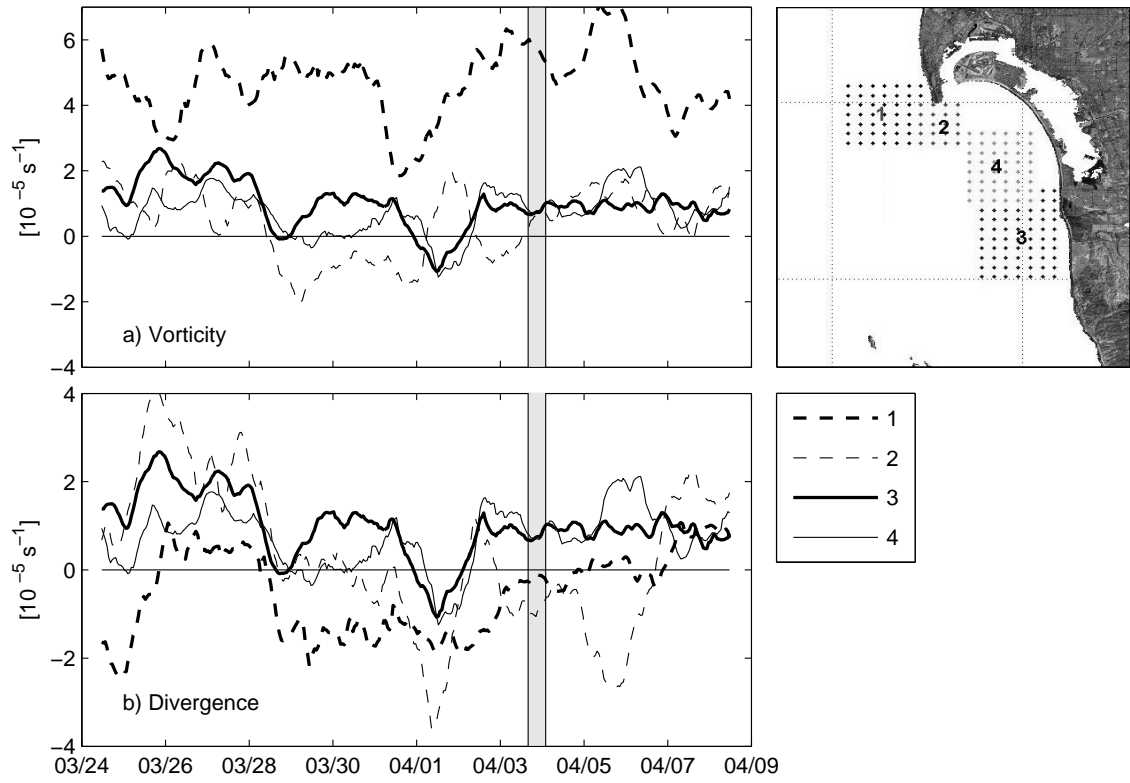
Figure 9: Time series of mean a) Vorticity and b) Divergence ($s^{-1} \times 10^{-5}$) at 4 regions. To the right is a map showing each of the regions.
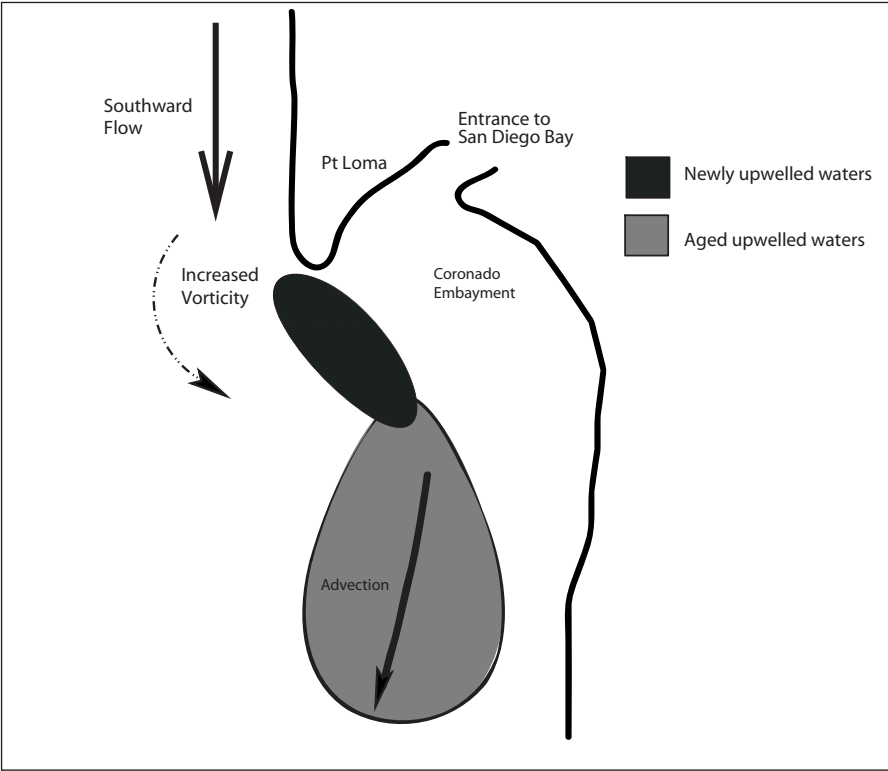
Figure 10: Schematic diagram of the circulation off the Pt Loma Headland.